https://doi.org/10.3311/PPci.22226

Periodica Polytechnica Civil Engineering, 67(4), pp. 1193–1202, 2023

Imperfections for Local and Global Interaction Buckling of Welded Square High-strength Steel Box-section Columns

Mohammad Radwan[1]*, Balázs Kövesdi[1]

[1] Department of Structural Engineering, Faculty of Civil Engineering, Budapest University of Technology and Economics, Műegyetem rkp. 3., 1111 Budapest, Hungary
* Corresponding author, e-mail: mohammad.radwan@emk.bme.hu

Received: 19 March 2023, Accepted: 19 June 2023, Published online: 17 July 2023

Abstract

The interaction behavior between local and global buckling modes in high-strength steel box-section columns has received limited research attention. Currently, there is a lack of a validated equivalent geometric imperfection that can be effectively employed in nonlinear plastic analysis to estimate the interaction buckling resistance. This research aims to find equivalent geometric imperfections that can be used in geometrical and materially nonlinear analysis using imperfections (GMNIA) to estimate the interaction buckling resistance of square welded box-section columns made of high-strength steel. It extends prior investigations by the authors on equivalent imperfections for normal-strength steel welded box-sections. A developed and validated numerical model is used to perform parametric studies to estimate the accurate buckling capacity using previously developed and verified combinations of imperfections and residual stresses. The accurate buckling capacities are used to calibrate equivalent local and global imperfection combinations that can be used in FEM-based design. A reliability assessment study is also performed to check the safety level of the proposed imperfection combinations.

Keywords

local buckling, flexural buckling, welded box-section, interaction buckling, equivalent imperfections, high strength steel

1 Introduction

Welded box-section columns are widely used in buildings and bridges due to their strength and stability. However, when these columns are subjected to compressive loads, they can fail due to global buckling, local buckling, or under the interaction of both. This significantly reduces the column's load-carrying capacity and compromises the structure's integrity. Global buckling involves the buckling of the entire column, while local buckling occurs when plates of the column cross-section fail due to compressive load. Interaction buckling occurs when both local and global buckling happens simultaneously. Globally and locally, slender sections are prone to this type of buckling. This study aims to find suitable equivalent imperfection combinations that can be used in numerical models to accurately estimate the interaction buckling resistance of welded square box-section columns made of high-strength steel (HSS). These combinations can be used in design problems not entirely covered by the current design standards.

Nonlinear analysis techniques, such as finite element analysis (FEA), can be used to simulate and predict the buckling behavior of columns. The combination of geometrical and material nonlinear analysis with imperfection (GMNIA) is particularly important, as it allows for more accurate predictions of the buckling capacity. Two possible techniques can be followed to perform GMNI analysis, either by using geometric imperfection and residual stresses or using equivalent geometric imperfections. Equivalent imperfection presents a more convenient way to perform GMNI analysis as these imperfections also take the effect of residual stresses, enabling the designer to avoid modeling the residual stresses that can be challenging for complex structures. Therefore, in this study, the magnitudes of equivalent geometric imperfections are determined by calibrating against the resistance obtained by modeling the residual stresses.

The authors extensively investigated the interaction buckling resistance of welded box-section columns in the past, where combinations of global and local imperfections with residual stresses were developed [1]. These combinations can accurately estimate the interaction buckling resistance of welded box-section columns. In these combinations, the authors calibrated local imperfections based

Cite this article as: Radwan, M., Kövesdi, B. "Imperfections for Local and Global Interaction Buckling of Welded Square High-strength Steel Box-section Columns", Periodica Polytechnica Civil Engineering, 67(4), pp. 1193–1202, 2023. https://doi.org/10.3311/PPci.22226

on the buckling curve of Schillo et al. [2] and Annex B of EN1993-1-5 [3–5]. These buckling curves were proven experimentally and numerically to better estimate the local buckling resistance of welded box-sections compared to the Winter-type buckling curve of the Eurocode EN 1993-1-1 [5–8]. The global imperfection used in the developed combination is L/1000, a widely agreed-upon imperfection if the residual stresses are applied [2]. Equivalent global imperfections suitable for GMNIA analysis were recently developed by Somodi et al. [9] for global buckling resistance. For interaction buckling, the authors developed equivalent imperfection combinations for welded square box-sections made of normal strength steel (NSS) [10]. However, several researchers emphasized the difference between normal and high-strength steel, such as residual stresses and material behavior [11]. Therefore, this research will develop equivalent imperfection combinations for high-strength steel welded box-section columns which are still missing from the international literature.

The current investigation uses the previously developed and validated numerical model to conduct a parametric study to find the accurate buckling resistance of square welded box-sections made of HSS. The accurate buckling resistance is determined using the previously developed combination of local and global imperfection with residual stresses for steel S500, S690, and S960 on a wide range of global and local slenderness. This resistance is considered reference resistance. A calibration process is performed to find equivalent global and local imperfections that yield buckling resistance equal to the reference resistance. After it, a detailed reliability assessment is performed to check the applicability of the calibrated imperfections and the safety margins.

The paper is organized into six chapters: Section 2 presents a comprehensive literature review on interaction buckling behavior, as well as the magnitudes of local and global imperfections. In Section 3, the development of a numerical model is discussed. Section 4 presents the results of parametric studies, demonstrating the calibrated equivalent global and local geometrical imperfections. Section 5 shows a detailed reliability analysis to evaluate the calibrated imperfection combinations. Finally, Section 6 examines the constant amplitude imperfection factors.

Overall, this paper serves as a resource for researchers and designers working in the field of FEM-based design to aid in estimating the interaction buckling resistance of HSS welded box-section columns.

2 Literature review

2.1 Interaction buckling resistance

Degée et al. [12] performed experiments on rectangular box-section columns made of S355 steel to study the interaction buckling resistance. An experimental test program has been executed on six specimens within a global slenderness range of $\bar{\lambda}_g$ = 0.35, 0.55, and 0.7 with constant local slenderness of $\bar{\lambda}_h$ = 0.9. L/1000 was used as global imperfection and b/1000 as local imperfection with applied residual stress in the numerical model. The authors found that the buckling curve "b" of EN 1993-1-1 [8] yields conservative results, and the buckling curve "a" had a better agreement. An enhanced design method was proposed that takes into account the loss of stiffness caused by local buckling, where a modified global slenderness ratio $\bar{\lambda}_{int}$ is determined, which depends on the gross to the effective moment of inertia and area and the local reduction factor ρ. In this method, higher resistance is estimated as λ_{int} is smaller than λ_g. Khan et al. [13] performed experiments on S690 welded box section columns to study the interaction buckling resistance. They performed an experimental test program on fifteen specimens, and a numerical study was performed. In the parametric study, the authors used L/1000 and b/1000 for global and local imperfections, respectively. Residual stresses were applied too. Specimens with intermediate lengths experienced global and local buckling. The authors suggested a reduction factor to consider the interaction effect, and the buckling curve "b" of EN1993-1-1[8] was suggested, as all the numerical results lay above it. Usami and Fukumoto [14] experimented on HSS S460 and S960 welded box-sections to study the interaction buckling capacity. Twenty-seven compression tests were performed, with twenty-four tests loaded concentrically and the remaining loaded eccentrically. Schillo et al. [2] conducted thirteen buckling tests on welded box-sections made of S500 and S960 to study the interaction buckling resistance. A numerical model was validated using the experimental tests, and a parametric study was conducted to determine reduction factors to determine the interaction resistance. The authors used the EN1993-1-1 [8] method to determine buckling resistance with an additional modification to account for stiffness loss caused by local buckling by including an equivalent local imperfection (e_p) in the reduction formula.

Somodi et al. [9] calibrated equivalent global imperfections based on EN1993-1-1 [8] buckling curves using a parametric study and GMNI analysis. An equivalent imper-

fection formula, denoted as L/f_{glob}, was proposed. The value of f_{glob} is determined according to Eq. (1), where $\varepsilon = \sqrt{\frac{235}{f_y}}$, α is the imperfection factor according to EN1993-1-1 [8], and $\bar{\lambda}_g = \sqrt{\frac{Af_y}{N_{cr}}}$ is the global slenderness ratio. The formula can be used for steel grades of S235-S960. It was found that the buckling resistance obtained using this formula showed good agreement with the buckling curves of the Eurocode. A maximum error of 2% was observed.

$$f_{glob} = \frac{\varepsilon}{\alpha}\left(\bar{\lambda}_g^{-3.8} - 26 \cdot \bar{\lambda}_g + 168\right) \quad (1)$$

Radwan and Kövesdi [5] calibrated local imperfections to fit the buckling curve of Annex B of EN1993-1-5 [4] and the curve developed by Schillo et al. [2]. The authors calibrated geometrical imperfections applied with residual stresses and equivalent geometrical imperfections that take the residual stresses into account. The imperfections mainly depend on the yield strength f_y and the local slenderness ratio $\bar{\lambda}_p$ of the analysed cross-section. The equivalent local imperfection can be determined based on Eq. (2), which represents accurate results compared to the calibrated imperfections for HSS. In Eq. (2), f_y is the nominal yield strength and $\bar{\lambda}_p$ is the local plate slenderness ratio. The local imperfection factor is applied as $b/f_{0,\text{local}}$, where b is the plate width. In a different study [15], the authors found that imperfection of b/125 yields resistances correspond with the buckling curve developed by Schillo et al. [2], based on statistical assessment with a mean value of 1.0.

$$f_{0,local} = \left(-0.3 \cdot f_y + 400\right) \cdot \bar{\lambda}_p^{-3.65} \quad (2)$$

2.2 Executed research strategy

Several researchers emphasized that further global and local buckling investigation is needed to estimate the buckling resistance accurately for welded box-sections made of HSS [2, 12, 16]. Moreover, new global and local equivalent imperfections must be developed for HSS to be used in the numerical modeling-based design, as the available suggestions are based on elastic analysis. Two shortcomings of the previous investigations on the interaction buckling are overcome in this study, where the buckling curve available in Annex B of EN1993-1-5 [4] is used instead of the Winter-type curve, which many researchers criticized for overestimating the local buckling resistance of welded box-sections. The other shortcoming is using a constant value for the local imperfections for the different sections with different steel grades and local slenderness. The authors developed local imperfections that depend on the steel type and local slenderness of each section under study, calibrated to Schillo et al. [2] and Annex B curves and yield their resistances if applied in the numerical model. This allows for a better estimation of the local buckling resistance.

This paper outlines the research program that was conducted and is being presented in the following manner:

1. The utilization of calibrated local geometric imperfection, as discussed in [5], enables control of the local buckling resistance to align with the Annex B curve of EN1993-1-5 [4]. A specific imperfection is used for each section depending on the yield strength and local slenderness ratio, as illustrated in Figure 19 of [5]. The manufacturing tolerance of $\pm b/125$ is used as the maximum applied imperfection [17] (max (calibrated imperfection to Annex B curve, b/125)).

2. The utilization of L/1000 as global imperfection with residual stresses enables control of the global buckling resistance. This imperfection magnitude yielded a good fit to the global buckling resistance [12, 18].

3. The previously developed and validated numerical model is used, as shown in the previous research [10], where this numerical model was validated for both NSS and HSS against tests in the literature.4. The numerical model and the combinations of imperfections and residual stresses are used to perform a parametric study to determine the accurate resistance (referred to as reference resistance) for a wide range of global and local slenderness ratios for steel grades of S500, S690, and S960.

5. Two additional numerical studies are performed to calibrate equivalent global and local imperfections. In the first parametric study, a leading local imperfection is chosen according to Eq. (2), and the global imperfections are calibrated. In the second parametric study, a leading global imperfection is chosen according to Eq. (1), and the local imperfections are calibrated. Calibrations are made to align with the reference buckling resistance.

3 The developed numerical model

Ansys finite element software [19] was utilized to develop the model using SHELL181 elements. Geometrical and material nonlinear analysis with imperfection (GMNIA) is used to estimate the buckling resistance of the columns under study. The global and local imperfections are defined in the numerical model, as shown in Fig. 1. The local imperfections are defined as half sin-waves, with alternative signs for adjacent edges, where outwards imperfections are considered positive, as shown in Fig. 1(a).

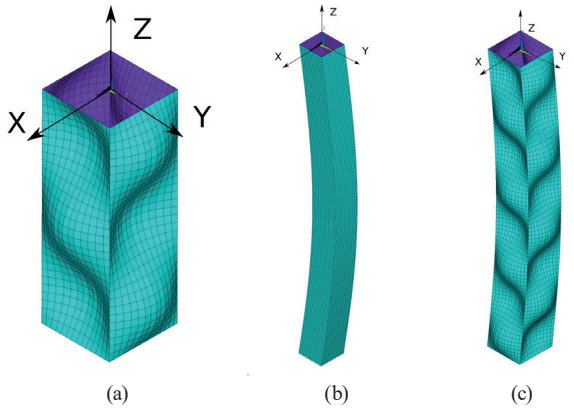

Fig. 1 Imperfection definition for columns experiencing (a) local, (b) global, (c) interaction buckling

The number of half sin-waves is equal to the length of the plate L divided by the plate width b. The global imperfection is applied as a large half sin-wave across the entire length of the column, as shown in Fig. 1(b). Both half sin-waves are applied in case of interaction buckling, as shown in Fig. 1(c). The accurate modeling of these imperfections is essential to ensure the efficient design of steel columns. Master nodes were added at the center of the end cross sections of the columns to define the boundary conditions and applied load. This simplifies the process of defining the boundary conditions. Rigid diaphragms are defined to link all 6 DOFs between the master nodes and end cross-section nodes. The translations in all directions (UX, UY, UZ) are restrained at the first master node, and the translation in X- and Y- directions (UX, UY) are restrained on the second node as the load is applied in the Z-direction. The rotation in the Z-direction (ROTZ) is restrained on both master nodes.

In contrast to NSS, where a quad-linear material model was used to define the behavior of the material, the Ramberg-Osgood-type material model is utilized in this research to define the material behavior for HSS, as depicted by Eq. (3). The model characterizes the nonlinear material behavior of HSS under complex loading conditions, such as large strains and stress reversals. This material model relates the stress and strain of the material by using the yield strength and the hardening exponent, which is determined by different coupon tests. In this analysis, a value of n = 14 is used with a modulus of elasticity of E = 210000 MPa and Poisson's ratio v = 0.3 [11]. The utilized yield and ultimate strengths are summarized in Table 1.

$$\varepsilon = \frac{\sigma}{E} + 0.002\left(\frac{\sigma}{fy}\right)^{n} \tag{3}$$

Table 1 The yield and ultimate strength of the studied HSS

Steel grade	Yield strength (f_y) [MPa]	Ultimate strength (f_u) [MPa]
S500	500	625
S690	690	850
S960	960	1115

The utilized residual stress model has been proven to provide an accurate estimation of buckling resistance and is consistent with the guidelines set forth by the European Convention for Constructional Steelworks (ECCS) [20] and the preliminary version of the updated Eurocode prEN1993-1-14 [21]. The sections studied in this investigation have an H/t ratio of 40 to study the interaction buckling of class 4 cross-sections. It was shown by several researchers that the compressive residual stresses have smaller values in HSS compared to NSS due to better welding techniques and manufacturing processes [22, 23]. Accordingly, the tensile residual stress is equal to the yield strength f_y, while the compressive residual stress is equal to 0.13 × 355 MPa for all the steel types in this study. Static equilibrium between residual stresses is used to define the tensile zone width.

Mesh sensitivity analysis is a numerical simulation technique for assessing the accuracy and reliability of finite element analysis (FEA) results. It involves systematically varying the mesh density of the model and analyzing the corresponding changes in the simulation results to determine the optimum mesh size for the analysis. In this research, it was found that a mesh of 16 elements along the plate width results in a reliable estimation of the resistance with 1% from the smallest applied mesh size. The details of the mesh analysis are illustrated in previous research [10]. Validation of the numerical model is a process of comparing the results obtained from numerical simulation with those obtained from physical experiments. It is essential to ensure the accuracy and reliability of the developed numerical model and its ability to predict the behavior of the test specimen. The details of the validation process of the numerical model are demonstrated in previous research [10], where the model was validated for both NSS and HSS using samples taken from several research programs with S235, S500, S700, and S960 steel types. The numerical model was able to estimate the buckling capacity of the test specimens accurately. The mean and coefficient of variation (CoV) of the ratio $\frac{F_{numerical}}{F_{experimantal}}$ is equal to 0.99 and 0.061, respectively.

$$Equivalent\ global\ imperfection = \frac{L}{f_{int}} \tag{4}$$

$$f_{int} = f_{glob} \cdot \begin{Bmatrix} \bar{\lambda}_p \le 0.7, \quad 1 \\ \bar{\lambda}_p \le 1.35, \quad 2 \cdot \bar{\lambda}_p - 0.4 \\ 1.35 < \bar{\lambda}_p \le 1.85, \quad 19.4 \cdot \bar{\lambda}_p - 23.9 \\ \bar{\lambda}_p > 1.85, \quad 12 \end{Bmatrix} \tag{5}$$

4 Results of the parametric studies

4.1 Equivalent global geometrical imperfection

In the first parametric study, the local imperfection is considered as leading imperfection applied with 100% magnitude depicted in Eq. (2), and the accompanying global imperfection is searched. The obtained equivalent global imperfections showed smaller differences between the studied HSS types. Hence, a single formula that fits all the investigated types is employed to calculate the equivalent global imperfection, as presented in Eqs. (4–5). The fit formula is expressed as f_{int}/f_{glob}, where f_{int} is the calibrated equivalent imperfection scaling factor and f_{glob} is the global imperfection scaling factor for pure global buckling according to Eq. (1). The accompanying imperfections are a function of local slenderness ratios. The proposed formula is illustrated in Fig. 2, depicting the relationship between the local slenderness ratio $\bar{\lambda}_p$ on the x-axis and the f_{int}/f_{glob} ratio on the y-axis for several global slenderness ratios $\bar{\lambda}_g$, shown in the legend. Fig. 2 demonstrates the global and local slenderness, where a smaller or equal imperfection is required in comparison to the pure global imperfections. No interaction occurs before $\bar{\lambda}_p < 0.7$, therefore f_{int}/f_{glob}, the is equal to 1.0, as shown in the Fig. 2. For $\bar{\lambda}_p < 1.35$, the ratio f_{int}/f_{glob} ratio is represented by a line with an increasing magnitude with a value less than 3.0. For the region $1.35 < \bar{\lambda}_p < 1.85$, the imperfection scaling factor is another line with a larger slope due to the fact that a relatively larger local imperfection was applied here, and therefore, a smaller accompanying global imperfection is required for this region. For local slenderness larger than $\bar{\lambda}_p > 1.85$, an upper limit of 12 was applied as the smallest possible applied accompanying imperfection to yield safe results. It is worth mentioning that different trends are obtained for HSS compared to NSS as different material models, local imperfections, and residual stress magnitudes are applied. The obtained equivalent global imperfection can be applied according to Eq. (4), where f_{int} is obtained using Eq. (5).

4.2 Equivalent local geometrical imperfection

This approach involves using the global imperfection as the leading imperfection with 100% magnitude and subsequently determining the magnitudes of local imperfections required for the analyzed cross-section against the reference buckling capacity. The same procedures, as shown in Section 4.1, are followed here using the same sections and materials properties. An accompanying equivalent local imperfection is proposed, as shown in Fig. 3, if Eq. (1) is employed as the leading global imperfection scaling factor.

Fig. 3 illustrates the global slenderness ratio $\bar{\lambda}_p$ on the x-axis and f_{int}/f_{loc} ratio on the y-axis. f_{int} is the obtained accompanying local imperfection scaling factor for columns experiencing interaction buckling. f_{loc} is the equivalent imperfection scaling factor for pure local buckling, as depicted by Eq. (2). Fig. 3 shows that there is a clear trend for the f_{int}/f_{loc}, where the ratio is smaller for small global slenderness ratio (large imperfection is needed) and larger for large global slenderness (small imperfection is needed). This is because the local imperfection is less significant for columns with high global slenderness. On the local slenderness range, the trend starts with a larger f_{int}/f_{loc} ratio decrease to a minimum around the range 1–1.2 and gradually increases for a larger local slenderness ratio indicating a small imperfection; this happens due to the

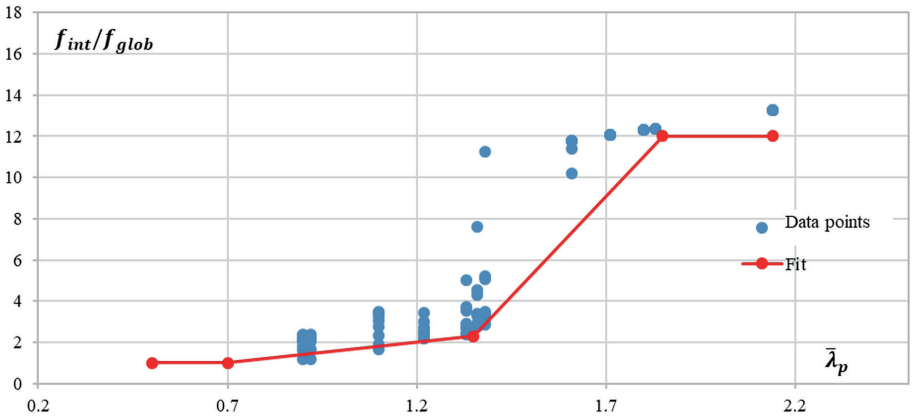

Fig. 2 Suggested formula for accompanying equivalent global imperfections

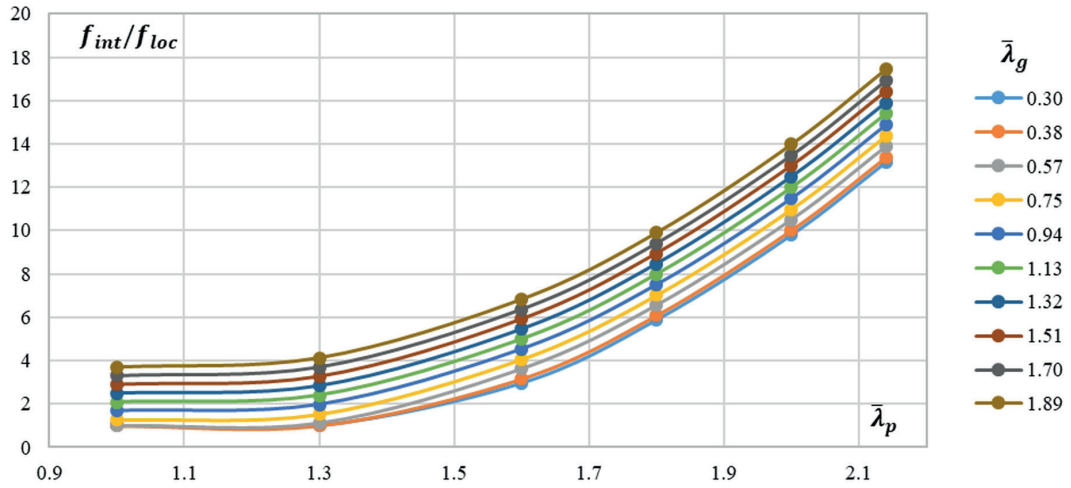

Fig. 3 Suggested formula for accompanying equivalent local imperfections

applied global imperfections where it is large for this range, and therefore to achieve the reference resistance only a smaller imperfection is needed. It was noticed that the differences in calibrated imperfections for the studied HSS are small. Therefore, a single equation can be used for all the studied HSS columns, as depicted by Eqs. (6)–(7). The calibrated accompanying equivalent local imperfection for interaction is according to Eq. (6), and f_{int} is according to Eq. (7).

$$Equivalent\ local\ imperfection = \frac{b}{f_{int}} \tag{6}$$

$$f_{int} = f_{local} \cdot \begin{cases} 1.0, \ \bar{\lambda}_p \le 1.3, \ \bar{\lambda}_g \le 0.6 \\ \left(12 - 19.8 \cdot \bar{\lambda}_p - 1.6 \cdot \bar{\lambda}_g + 8 \cdot \bar{\lambda}_p^2 + 2.6 \cdot \bar{\lambda}_p \cdot \bar{\lambda}_g\right) > 1.0, \ \bar{\lambda}_p > 1.3 \end{cases} \tag{7}$$

It is important to notice that this formula is only applicable to the range $\bar{\lambda}_p > 0.7$ and $\bar{\lambda}_g > 0.2$, where the interaction buckling occurs. It is worth noticing that for the range $0.9 < \bar{\lambda}_p < 1$ and $\bar{\lambda}_g > 1.12$ the required equivalent local imperfection is always smaller than $b/500$. When f_{int} is less than 500, utilizing solely the global imperfection in accordance with Eq. (1) results in overestimating the buckling capacity by less than 5%.

5 Evaluating the calibrated imperfection combinations using statistical assessment

This section presents the reliability assessment performed according to the method of the EN1990 Annex D [24]. The method aims to ensure that structural designs meet specified levels of reliability and safety, taking into account the uncertainties associated with various factors.

The reference resistance, determined using the developed combination of residual stresses and imperfections for HSS [5], accurately predicts the interaction buckling resistance of welded box sections. In this study, the reference resistance is considered as the experimental results r_e. The buckling resistance obtained using the previously obtained equivalent imperfection formulas in Section 4 is considered the theoretical resistance r_t. EN1990 Annex D [24] outlines a systematic approach for evaluating the reliability of structural systems in design. As per Eurocode standards, the corrected partial safety factor, γ_M^*, for member stability is set to 1.0 for buildings and 1.1 for bridges. To begin with Annex D method, a comparison is made between the experimental r_t (y-axis) and theoretical r_e (x-axis) resistances by plotting them as pairs, as illustrated in Fig. 4.

The detailed statistical evaluation to determine the partial safety factor was demonstrated in previous research by the authors [10]. Here, only a summary of the steps is presented. The model uncertainties must be determined by calculating the mean value correction factor b, the error term δ_i for each experimental resistance value, the variance s^2 and the coefficient of variations V_δ, according to [10]. The coefficient of variation V_δ is a measure of the variabilities in estimating the resistance using the proposed theoretical values. Several basic variables contribute to the uncertainties of the design method. In this study, the material strength f_y, the plate width b, the thickness t, and the length L are considered the main basic variables, shown in [10]. Smaller values for the V_{fy} are utilized here for HSS, as shown by Schillo et al. [2]. The general coefficient of variations V_{rt} ,which includes the CoVs of the basic variables, the coefficient of variations of the model

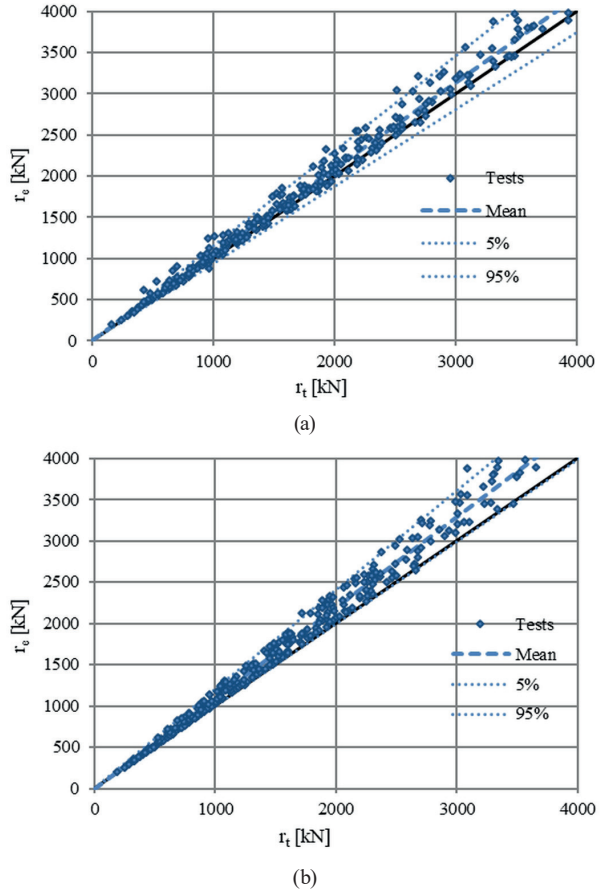

Fig. 4 The reference resistance re (experimental) and the equivalent imperfection combination resistance rt (theoretical). (a) Using leading local and accompanying global. (b) Using leading global and accompanying local

V_r and the partial safety factor γ_M can be determined according to [10]. Several researchers used the nominal values of the basic variables to determine a corrected partial safety factor, as they found that it yields a better prediction of the partial safety factor [2, 25–29]. A different method that is used by other researchers considers the Δk coefficient. Δk is a modification factor equal to the mean value of resistance calculated using nominal values to the characteristic values. Here the Δk coefficient method is used to find the corrected partial safety factor.

Table 2 summarizes the performed reliability assessments for the developed imperfection combinations (i) leading local and accompanying global and (ii) leading global and accompanying local. (iii) the minimum resistance obtained by (i) or (ii). The table shows the leading imperfection, the local imperfection scaling factor, the global imperfection scaling factor, the mean value correction bm, the coefficient of variations b_m, V_δ, $V_{rt,avg}$, $V_{r,avg}$ and the corrected partial safety factors γ_M^*. The total number of samples is 310.

Table 2 Summary of the parameter uncertainties using the nominal values and overstrength factor

Criteria	Local imp.	Global imp.	b_m	V_δ	$V_{rt,avg}$	$V_{r,avg}$	γ_M^*
Leading local	*b*/Eq. (2)	calib-rated	1.04	0.0598	0.0711	0.0929	1.116
Leading global	calib-rated	*L*/Eq. (1) - *b* curve	1.07	0.0543	0.0711	0.0895	1.000
Min			1.08	0.0464	0.0711	0.0849	1.000

As shown in Table 2, the mean correction factor b_m for both combinations is larger than 1.0, indicating that the resistance of the numerical model implementing the equivalent combinations of imperfections is smaller than the reference resistance, i.e., safe side results. If the uncertainties are considered, the achieved value for the leading local imperfection combination is 1.116, and for the leading global imperfection combination is 1.000. It can be seen that the combination leading global and calibrated accompanying local provides safe and reliable results with minimum scatter. A smaller scatter is achieved by taking the minimum resistance of the two combinations yielding safe results.

6 Constant amplitude imperfection factors

In accordance with Annex C of Eurocode EN1993-1-5 [4], when combining imperfections, a leading imperfection can be selected, and the accompanying imperfection may be reduced to 70%. In this parametric study, three combinations are tested; i) both global and local imperfections are applied with 100% magnitude, ii) the global imperfection is applied with 100%, and the local imperfection is reduced to 70%, iii) the local imperfection is applied with 100%, and the global imperfection is reduced to 70%. It was mentioned in the literature review that the authors found that the local imperfection *b*/125 yielded the best-fit estimation of the buckling curve developed by Schillo et al. [2]. By applying this imperfection in a numerical model, the obtained buckling resistance is close to the buckling resistance estimated by the mentioned buckling curve. Hence, this local imperfection is used here in the parametric study. For global imperfections, the formula developed by Somodi et al. [9, 30] is used for the global buckling imperfection scaling factor according to Eq. (1). The global imperfection is applied as the length *L* over the value obtained using Eq. (1).

The same statistical assessment procedures described in Section 5 are applied here to evaluate the computed resistances and obtain the corrected partial safety factors

for the discussed combinations of imperfections. The experimental resistance r_e is the reference resistance, and the resistance obtained with the mentioned combinations is the theoretical resistance r_t. Fig. 5 shows the outcomes of the parametric study. The figures compare the buckling resistance obtained using the studied combinations (theoretical resistance) to the reference resistance (experimental resistance). Fig. 5(a) depicts the combination where both global and local imperfections are set to 100% magnitude, Fig. 5(b) shows the combination with 70% reduction in local and 100% in global imperfection, while Fig. 5(c) shows the combination with 100% local and 70% global imperfection. The blue lines in the figures represent the 5% and 95% values. It can be seen that all three combinations yielded results within the 5% range around the mean value.

The same procedures shown previously are used to determine the parameters in Table 3. If both imperfections are applied with 100% magnitude, the mean correction factor equals to 1.11, indicating that the obtained average numerical results (r_t) are smaller than the reference resistance (r_e). All the other combinations yield safe resistance based on b_m. By taking the model uncertainties into account, it is possible to see that the corrected partial safety factors γ_M^* for 100% global and 100% local combination is less than 1.0 while all the other combinations are larger than 1.0; this happens since the b_m value is larger. It can be seen the scatter is large for constant imperfection combinations, as demonstrated by taking a look at the value of V_δ and comparing the values to Table 2. The larger value of the coefficient of variation is due to using a constant local imperfection factor instead of a curve. A smaller scatter can be achieved if the minimum resistance of 70% local and 70% global combinations is considered compared to each combination individually.

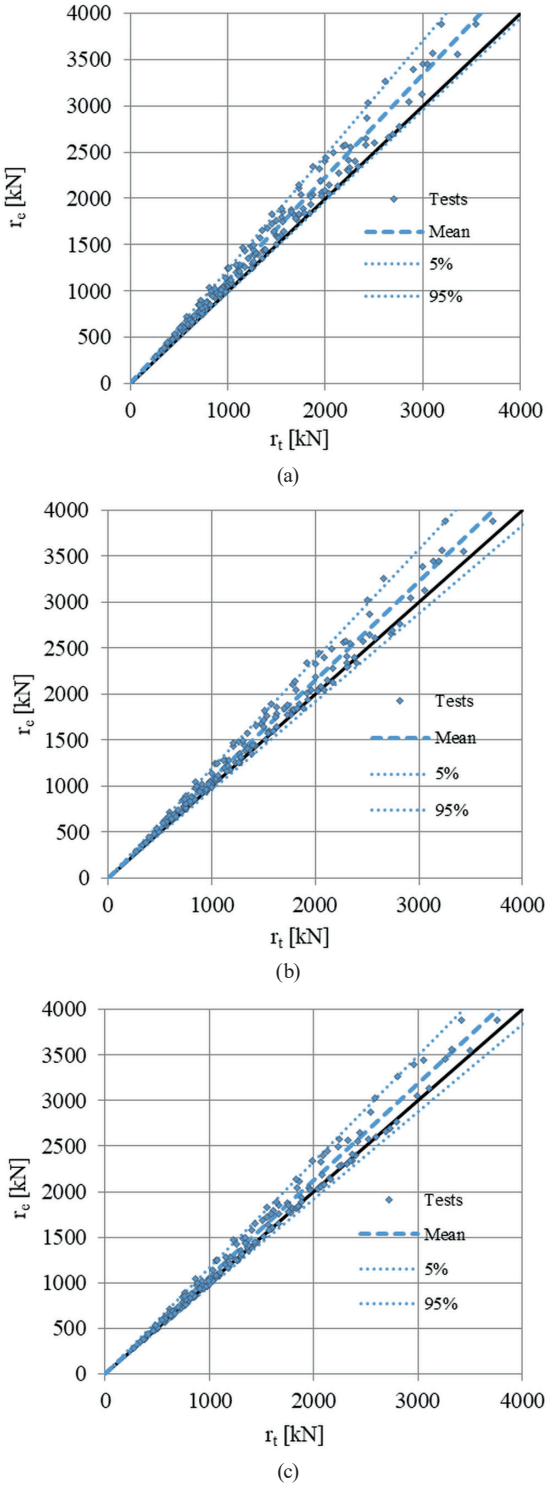

Fig. 5 The reference resistance re (experimental) and the equivalent imperfection combination resistance rt (theoretical). a) using 100% global and 100% local. b) using 100% global and 70% local. c) using 70% global and 100% local

7 Conclusions

Previous studies proved that the equivalent imperfection factors given by the Eurocode were developed for elastic analysis, and using them in GMNI analysis is not recommended. In previous research, the authors developed equivalent local and global imperfection combinations that can be used to estimate the buckling resistance of square welded box-sections experiencing interaction buckling [10]. However, these imperfections were developed mainly for normal-strength steel (NSS). Therefore, this research used the same approach to develop equivalent imperfection combinations suitable for welded box-sections made of high-strength steel (HSS). The equivalent imperfections are calibrated against a reference resistance obtained by combining local and global imperfections with residual stresses that the authors developed in a different research study [1]. Equivalent local and global

Table 3 Summary of the parameter uncertainties using the nominal values and overstrength factor for S500, S690, and S960

Criteria	Local imp.	Global imp.	b_m	V_δ	V_{rt}	V_r	γ_M^*
70% local	$0.7 \cdot \frac{b}{125}$	$\frac{L}{\text{Eq.(1)}}$	1.08	0.063	0.071	0.095	1.06
70% global	$\frac{b}{125}$	$0.7 \cdot \frac{L}{\text{Eq.(1)}}$	1.06	0.056	0.071	0.091	1.073
Min (70%local, 0%global)			1.08	0.062	0.071	0.094	1.051
100% global and 100% local	$\frac{b}{125}$	$\frac{L}{\text{Eq.(1)}}$	1.11	0.065	0.071	0.096	0.998

imperfections were previously determined for pure local and global buckling modes [5, 30]. A leading imperfection using the pure local or pure global imperfection is selected, and the accompanying imperfection is calibrated against the reference resistance. A reliability assessment study was conducted to check if the obtained combinations of leading and accompanying imperfections meet the safety requirements of Annex D of EN1990 [29]. The study showed that the proposed equivalent imperfection combinations provide safe results based on the mean correction factor b_m. By taking the uncertainness into account, the analysis revealed that by taking the global imperfection as the leading imperfection, a partial correction factor of γ_M* 1.00 is obtained for the full set, including S500, S690 and S960, which can be safely used for design. However, the combination with local imperfection is the leading imperfection yield a partial safety factor γ_M* of 1.12 for the full set.

Annex C of Eurocode EN1993-1-5 [4] recommends choosing a leading imperfection, applied with 100% magnitude, and the accompanying imperfection magnitude reduced to 70%. Two additional parametric studies were conducted to investigate the applicability of this suggestion, using equivalent global and constant local imperfections. The findings demonstrated that while it is generally safer to employ 100% magnitude of both global and local imperfections. However, the difference in the average resistance using 70% or 100% for the accompanying imperfection leads to a maximum of 3% difference. Therefore, it is recommended to use 100% for both imperfection types in the design practice; thus, it does not lead to large differences.

In summary, this paper has developed and validated equivalent geometrical imperfections for accurately estimating the interaction buckling resistance of square welded box sections made of high-strength steel, specifically tailored for use in GMNIA. These findings significantly contribute to enhancing FEM-based design practices.

Acknowledgment

The presented research program has been financially supported by the Grant MTA-BME Lendület LP2021-06/2021 "Theory of new generation steel bridges" program of the Hungarian Academy of Sciences and Stipendium Hungaricum Scholarship. Both grants are gratefully acknowledged.

References

[1] Radwan, M., Kövesdi, B. "Improved design method for interaction buckling resistance of welded box-section columns", Journal of Constructional Steel Research, 194, 107334, 2022. https://doi.org/10.1016/j.jcsr.2022.107334

[2] Schillo, N., Feldmann, M., Taras, A. "Local and Global Buckling of Box Columns Made of High Strength Steel", PhD Thesis, RWTH Aachen University, 2017.

[3] Radwan, M., Kövesdi, B. "Equivalent Geometric Imperfections for Local Buckling of Slender Box-section Columns", Periodica Polytechnica Civil Engineering, 65(4), pp. 1279–1287, 2021. https://doi.org/10.3311/PPci.18545

[4] CEN "EN 1993-1-5:2006. Eurocode 3-Design of steel structures, Part 1.5: Plated structural elements", European Committee for Standardization, Brussels, Belgium, 2006.

[5] Radwan, M., Kövesdi, B. "Local plate buckling type imperfections for NSS and HSS welded box-section columns", Structures, 34, pp. 2628–2643, 2021. https://doi.org/10.1016/j.istruc.2021.09.011

[6] Schillo, N., Taras, A., Feldmann, M. "Assessing the reliability of local buckling of plates for mild and high strength steels", Journal of Constructional Steel Research, 142, pp. 86–98, 2018. https://doi.org/10.1016/j.jcsr.2017.12.001

[7] Clarin, M. "High strength steel: local buckling and residual stresses", Licentiate Thesis, Luleå University of Technology, 2004. [online] Available at: http://www.diva-portal.org/smash/record.jsf?pid=diva2%3A990619&dswid=4129

[8] CEN "EN 1993-1-1:2005. Eurocode 3: Design of steel structures - Part 1-1: General rules and rules for buildings", European Committee for Standardization, Brussels, Belgium, 2005.

[9] Somodi, B., Bärnkopf, E., Kövesdi, B. "Applicable Equivalent Bow Imperfections in GMNIA for Eurocode Buckling Curves – in Case of Box Sections", ce/papers, 5(4), pp. 563–567, 2022. https://doi.org/10.1002/cepa.1791

[10] Radwan, M., Kövesdi, B. "Equivalent geometrical imperfections for local and global interaction buckling of welded square box section columns", Structures, 48, pp. 1403–1419, 2023. https://doi.org/10.1016/j.istruc.2023.01.045

[11] Somodi, B. "Flexural buckling resistance of high strength steel welded and cold-formed square closed section columns", PhD Thesis, Budapest University of Technology and Economics, 2017. [online] Available at: http://hdl.handle.net/10890/5517

[12] Degée, H., Detzel, A., Kuhlmann, U. "Interaction of global and local buckling in welded RHS compression members", International Colloquium on Stability and Ductility of Steel Structures, 64(7), pp. 755–765, 2008. https://doi.org/10.1016/j.jcsr.2008.01.032

[13] Khan, M., Uy, B., Tao, Z., Mashiri, F. "Concentrically loaded slender square hollow and composite columns incorporating high strength properties", Engineering Structures, 131, pp. 69–89, 2017. https://doi.org/10.1016/j.engstruct.2016.10.015

[14] Usami, T., Fukumoto, Y. "Local and overall buckling of welded box columns", Journal of the Structural Division, 108(3), pp. 525–542, 1982. https://doi.org/10.1061/JSDEAG.0005901

[15] Radwan, M., Kövesdi, B. "Equivalent local imperfections for FEM-based design of welded box sections", Journal of Constructional Steel Research, 199, 107636, 2022. https://doi.org/10.1016/j.jcsr.2022.107636

[16] Kwon, Y. B., Seo, E. G. "Prediction of the compressive strength of welded RHS columns undergoing buckling interaction", Thin-Walled Structures, 68, pp. 141–155, 2013. https://doi.org/10.1016/j.tws.2013.03.009

[17] BSI "EN 1090-2:2018. Execution of steel structures and aluminium structures - Part 2: Technical requirements for steel structures", British Standards Institution, London, UK, 2005.

[18] Johansson, B., Maquoi, R., Sedlacek, G., Müller, C., Beg, D. "Commentary and worked examples to EN 1993-1-5 "Plated structural elements"", European Commission, JRC scientific and technical reports, 2007.

[19] Ansys "ANSYS® v18", 2021.

[20] ECCS "European recommendations for steel construction; buckling of steel shells. European Convention for Constructional Steelwork", Brussels, Belgium, 1988.

[21] CEN "prEN 1993-1-14:2020. Eurocode 3: Design of steel structures, Part 1-14: Design assisted by Finite element analysis (under development)", European Committee for Standardization, Brussels, Belgium, 2021.

[22] Khan, M., Paradowska, A., Uy, B., Mashiri, F., Tao, Z. "Residual stresses in high strength steel welded box sections", Journal of Constructional Steel Research, 116, pp. 55–64, 2016. https://doi.org/10.1016/j.jcsr.2015.08.033

[23] Wang, Y.-B., Li, G.-Q., Chen, S.-W. "The assessment of residual stresses in welded high strength steel box sections", Journal of Constructional Steel Research, 76, pp. 93–99, 2012. https://doi.org/10.1016/j.jcsr.2012.03.025

[24] CEN "EN1990:2002. Eurocode—Basis of structural design", European Committee for Standardization, Brussels, Belgium, 2002.

[25] Taras, A., da Silva, L. S. "European Recommendations for the Safety Assessment of Stability Design Rules for Steel Structures", ECCS Technical Committee, Brussels, Belgium, Doc. ECCS–TC8-2012–06–XXX, 2012.

[26] Simões da Silva, L., Tankova, T., Marques, L., Rebelo, C. "Comparative Assessment of semi-probalistic methodologies for the safety assessment of stability design rules in the framework of annex D of EN 1990", University of Coimbra, Doc. ECCS–TC8-2013–11–024, 2014.

[27] Walport, F., Gardner, L., Nethercot, D. A. "Equivalent bow imperfections for use in design by second order inelastic analysis", Structures, 26, pp. 670–685, 2020. https://doi.org/10.1016/j.istruc.2020.03.065

[28] Heinisuo, M. "Axial resistance of double grade (S355, S420) hollow sections manufactured by SSAB", In: Design guides for high strength structural hollow sections manufactured by SSAB–for EN 1090 applications, Tampere University of Technology, Tampere, Finland, 2014.

[29] Taras, A., Huemer, S. "On the influence of the load sequence on the structural reliability of steel members and frames", Structures, 4, pp. 91–104, 2015. https://doi.org/10.1016/j.istruc.2015.10.007

[30] Somodi, B., Bärnkopf, E., Kövesdi, B. "Applicable equivalent bow imperfections in GMNIA for Eurocode buckling curves – SHS, RHS and welded box sections", Journal of Constructional Steel Research, 204, 107860, 2023. https://doi.org/10.1016/j.jcsr.2023.107860